LETTER

doi:10.1038/nature13388

Direct high-precision measurement of the magnetic moment of the proton

A. Mooser[1,2]†, S. Ulmer[3], K. Blaum[4], K. Franke[3,4], H. Kracke[1,2], C. Leiteritz[1], W. Quint[5,6], C. C. Rodegheri[1,4], C. Smorra[3] & J. Walz[1,2]

One of the fundamental properties of the proton is its magnetic moment, μ_p. So far μ_p has been measured only indirectly, by analysing the spectrum of an atomic hydrogen maser in a magnetic field[1]. Here we report the direct high-precision measurement of the magnetic moment of a single proton using the double Penning-trap technique[2]. We drive proton-spin quantum jumps by a magnetic radio-frequency field in a Penning trap with a homogeneous magnetic field. The induced spin transitions are detected in a second trap with a strong superimposed magnetic inhomogeneity[3]. This enables the measurement of the spin-flip probability as a function of the drive frequency. In each measurement the proton's cyclotron frequency is used to determine the magnetic field of the trap. From the normalized resonance curve, we extract the particle's magnetic moment in terms of the nuclear magneton: $\mu_p = 2.792847350(9)\mu_N$. This measurement outperforms previous Penning-trap measurements[4,5] in terms of precision by a factor of about 760. It improves the precision of the forty-year-old indirect measurement, in which significant theoretical bound state corrections[6] were required to obtain μ_p, by a factor of 3. By application of this method to the antiproton magnetic moment, the fractional precision of the recently reported value[7] can be improved by a factor of at least 1,000. Combined with the present result, this will provide a stringent test of matter/antimatter symmetry with baryons[8].

The challenge to measure the properties of the proton with great precision inspires very different branches of physics. As part of the intense search for baryon number violation so far, a lower limit of the proton's lifetime of $t_p > 2.1 \times 10^{29}$ years has been set[9]. Employing Penning traps, the proton's atomic mass was measured with a fractional precision of 0.14 parts per billion (p.p.b.; ref. 10), and the proton-to-electron mass ratio was determined with a relative accuracy of 94 parts in 10^{12} (ref. 11). Both provide essential input parameters with which to test the theory of quantum electrodynamics and contribute to the search for physics beyond the Standard Model. Furthermore, exciting results obtained by spectroscopy of muonic hydrogen[12] yielded a new value of the proton charge radius, and compared to previous measurements a 7σ deviation was observed, which has yet to be understood.

Another property of the proton is its spin magnetic moment

$$\mu_p = g_p \frac{q_p}{2m_p} S \qquad (1)$$

where q_p/m_p is the charge-to-mass ratio and S is the particle's spin. The constant g_p is a dimensionless measure of μ_p in units of the nuclear magneton $\mu_N = q_p\hbar/(2m_p)$, where $\hbar$ is the reduced Planck constant. The most precise value of μ_p (see Fig. 1, white bar) is extracted from spectroscopy of atomic hydrogen[1]. In this experiment the bound proton-to-electron magnetic moment ratio $\mu_p(H)/\mu_e(H)$ was measured with a fractional precision of 10 p.p.b., and μ_p was calculated by taking theoretical corrections at the level of about 18 parts per million into account[6].

A scheme for the direct measurement of magnetic moments of single particles in Penning traps has been applied with great success in measurements of the $g-2$ values (where g is the dimensionless measure of the electron magnetic moment μ_e in units of the Bohr magneton $\mu_B = q_e\hbar/(2m_e)$) of the electron and the positron[13] and further improved for the electron in ref. 14, where fractional precisions at the level of 3.8 and 0.28 parts in 10^{12} were achieved, respectively. The application of this scheme to measure the magnetic moment of the proton is a considerable challenge, because μ_p is about 658 times smaller than the magnetic moment of the electron μ_e. Thus, an apparatus with much higher sensitivity to the magnetic moment is needed.

In a Penning trap, the g-factor of the proton is determined by the measurement of a frequency ratio $g_p/2 = \nu_L/\nu_c$ where $\nu_c = q_pB_0/(2\pi m_p)$ is the cyclotron frequency, and $\nu_L = (g_p/2)\nu_c$ is the spin-precession frequency, also called the Larmor frequency. Both frequencies are measured in the same magnetic field B_0. The cyclotron frequency is obtained by the Brown–Gabrielse invariance theorem, $\nu_c^2 = \nu_+^2 + \nu_z^2 + \nu_-^2$, where ν_+, ν_z and ν_- are the characteristic oscillation frequencies of the trapped particle[15], the modified cyclotron frequency, the axial frequency and the magnetron frequency, respectively. The Larmor frequency can be measured by application of the so-called continuous Stern–Gerlach-effect[3]. In that scheme a magnetic field inhomogeneity $\Delta B(z)_z = B_2z^2$ is superimposed on the trap, where B_2 characterizes its strength and z is the axial coordinate. This 'magnetic bottle' couples the spin magnetic moment to the axial oscillation frequency, thus reducing the determination of the spin state to a measurement of ν_z. A spin-flip shifts the axial frequency by $\Delta\nu_{z,SF} = (\mu_pB_2)/(2\pi^2m_p\nu_z)$. This enables the measurement of the spin transition rate as a function of an applied drive frequency ν_{rf}, and yields the Larmor frequency ν_L (ref. 16).

In our experiment, we use $B_2 = 2.97(10) \times 10^5\,\mathrm{T\,m^{-2}}$ (ref. 4), which is 2,000 times stronger than in the electron/positron experiments[13]. In the presence of such a strong magnetic inhomogeneity the axial frequency shift caused by a spin-transition is $\Delta\nu_{z,SF} = 171$ mHz out of $\nu_z \approx 740$ kHz. Thus, the detection of proton spin quantum jumps requires an adequate axial frequency stability that is difficult to achieve in the strong magnetic bottle B_2 (ref. 17). However, dramatic progress in the manipulation of a single trapped proton allowed the first direct measurements of the proton magnetic moment μ_p (refs 4 and 5; see Fig. 1, grey bars). Those experiments were carried out solely in Penning traps with a superimposed B_2, which are usually called 'analysis traps'. The strong inhomogeneity broadens the width of the spin resonance, and ultimately limits the precision to the level of parts per million. An elegant solution to boost experimental precision is provided by the double Penning-trap technique[2]. This method separates the analysis of the spin state from the precision measurements of ν_c and ν_L. In addition to the analysis trap, a precision trap is used, in which the magnetic field is more homogeneous by orders of magnitude. This narrows the width of the Larmor resonance dramatically, and thus improves the precision. Here we report the first direct measurement of the proton magnetic moment using this technique.

Figure 2a shows a schematic of our double Penning-trap setup located at the University of Mainz, Germany. It is mounted in the horizontal and southward-oriented bore of a superconducting magnet, with a magnetic field of $B_0 \approx 1.89$ T and a stability of $(\Delta B/B_0)/\Delta t = 4.0(0.7) \times 10^{-9}\,\mathrm{h^{-1}}$.

[1]Institut für Physik, Johannes Gutenberg-Universität Mainz, 55099 Mainz, Germany. [2]Helmholtz-Institut Mainz, 55099 Mainz, Germany. [3]RIKEN, Ulmer Initiative Research Unit, Wako, Saitama 351-0198, Japan. [4]Max-Planck-Institut für Kernphysik, 69117 Heidelberg, Germany. [5]Fakultät für Physik und Astronomie, Ruprecht-Karls-Universität Heidelberg, 69047 Heidelberg, Germany. [6]GSI—Helmholtzzentrum für Schwerionenforschung, 64291 Darmstadt, Germany. †Present address: RIKEN, Ulmer Initiative Research Unit, Wako, Saitama 351-0198, Japan.

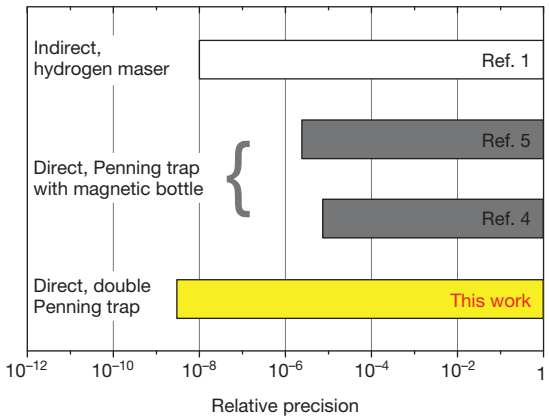

Figure 1 | Relative precision achieved in measurements of the proton magnetic moment. The value extracted indirectly from measurements with a hydrogen maser has a precision of 10 p.p.b. (ref. 1). Direct measurements with a single proton in a Penning trap with strong superimposed magnetic inhomogeneities were performed in 2012 by us[4] and a group at Harvard[5]. The result of the measurement described in this work was achieved by using the double Penning-trap technique with a single trapped proton. Our result is 3 times more precise than reported in ref. 1 and about 760 times more precise than other direct single particle measurements.

Each trap consists of five stacked cylindrical electrodes. The central ring electrode of the analysis trap is made out of ferromagnetic Co/Fe material, which generates the magnetic bottle. The other electrodes are made out of oxygen-free copper. To prevent oxidation all electrodes are gold-plated. The two trap centres are separated by 43.7 mm. Within this distance the magnetic-field inhomogeneity drops significantly. In the precision trap (PT) we have $B_{PT} = B_0 + B_{1,PT}z + B_{2,PT}z^2$, where $B_{1,PT} \approx 85\ \mathrm{T\,m^{-1}}$ and $B_{2,PT} \approx 4\ \mathrm{T\,m^{-2}}$, which is 75,000 times smaller than in the analysis trap. To shuttle the particle from one trap to the other, potential ramps are applied to transport electrodes located between the two traps. Radio-frequency drives applied to coils mounted close to each trap generate oscillating magnetic fields to drive proton spin transitions. The entire setup is placed in a hermetically sealed vacuum chamber cooled to 4 K. In this chamber pressures below 10^{-14} Pa are achieved[18], providing single-proton storage times of at least one year.

Protons are produced with an in-trap electron impact ion source. Electrons from a field emission gun hit a polyethylene target. Sputtered atoms are ionized in the centre of the precision trap. From the loaded ion-cloud a single proton is prepared using well established techniques[19].

Once a single proton is prepared, the particle's modified cyclotron mode is cooled resistively. This is achieved by tuning a cryogenic tank circuit, which acts on resonance as a resistor, to the cyclotron mode at $\nu_+ = 28.9$ MHz (ref. 20). Subsequently, the particle is shuttled to the analysis trap and the axial frequency is measured. To this end, $\nu_z \propto \sqrt{V_0}$ is tuned to resonance with our superconducting axial detection system at 740 kHz by adjusting the trapping voltage V_0. Once the axial motion is cooled to thermal equilibrium, the particle shorts the thermal noise of the detector and appears as a dip in the fast Fourier transform of the detector signal[21]. Such a fast Fourier transform spectrum is recorded in 60 s (shown as red points in Fig. 2b). By applying a fit to the data, the axial frequency ν_z is obtained. From this measurement, the quantum number of the cyclotron mode n_+ is determined[22]. Low n_+ is crucial to achieve an axial frequency stability which is sufficient to resolve single spin transitions[23,24]. Below a threshold cyclotron quantum number $n_{+,\mathrm{th}} < 1{,}500$ we achieve single spin-flip resolution with a fidelity

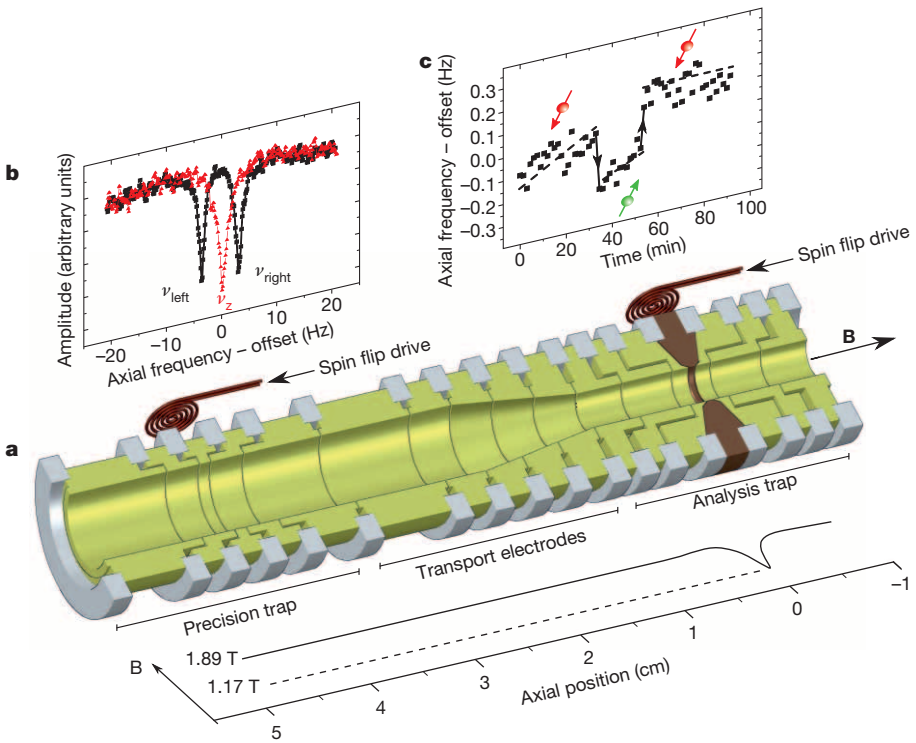

Figure 2 | Experimental setup and measurement procedures. a, Schematic of the double Penning-trap setup that is used for the direct measurement of the proton magnetic moment. It consists of two traps, an analysis trap and a precision trap, which are connected by transport electrodes. A strong magnetic field inhomogeneity is superimposed on the analysis trap, which is required to detect proton spin quantum transitions. In the precision trap, where the magnetic field is homogeneous, the precise frequency measurements are carried out. The solid curve in the plot below the trap system indicates the strength of the on-axis magnetic field. **b**, Fast Fourier transform spectrum of the axial detector's output signal. The dip (red) is due to a single particle, which shorts the thermal noise of the detector. The double-dip signal (black) appears when a quadrupolar sideband drive at $\nu_+ - \nu_z$ is applied. From such dip spectra ν_+, ν_z and ν_- are determined and thus the cyclotron frequency. The axial frequency has been offset by 623,850 Hz. For further details see text. **c**, Axial frequency measurement as a function of time. Frequency jumps of about 170 mHz are observed, which are due to induced single-proton spin transitions. The axial frequency has been offset by 742,060 Hz.

$F > 75\%$. This means that three out of four spin transitions are identified correctly. If $n_+ > n_{+,\mathrm{th}}$ is obtained, the particle is shuttled back to the precision trap and the cyclotron mode is cooled again. This procedure is repeated until $n_+ < n_{+,\mathrm{th}}$, which takes about two hours.

Once a particle with adequate n_+ is prepared, the actual g-factor measurement is conducted. First, the proton's spin state is identified. To this end, the axial frequency is measured and a spin-transition is induced by applying a magnetic radio-frequency drive, followed by another measurement of ν_z. As soon as a spin quantum jump is observed (see Fig. 2c), the proton's spin state is known. Afterwards, the particle is transported to the precision trap, where its cyclotron frequency ν_c is determined. First, the modified cyclotron frequency is measured via sideband coupling. An electric field at ν_{sb}, which is close to $\nu_+ - \nu_{z,\mathrm{PT}}$ is applied. This transfers energy between the axial mode and the modified cyclotron mode, and leads to a modulation of the axial oscillation amplitude. In the corresponding fast Fourier transform spectrum a so-called 'double-dip' with frequencies ν_{left} and ν_{right} for the left and the right dip, respectively, is observed (shown as black data points in Fig. 2b). Subsequently, the axial frequency is recorded, which is about $\nu_{z,\mathrm{PT}} \approx 624$ kHz. We determine ν_+ by applying the relation[25]

$$\nu_+ = \nu_{\mathrm{sb}} + \nu_{\mathrm{left}} + \nu_{\mathrm{right}} - \nu_{z,\mathrm{PT}} \quad (2)$$

The magnetron frequency $\nu_- \approx 7$ kHz is measured in a similar way. Finally, $\nu_{c,1}$ is obtained using the invariance theorem[15]. Next, spin transitions are induced by applying a spin-flip drive at $\nu_{\mathrm{rf,PT}}$ and subsequently the cyclotron frequency $\nu_{c,2}$ is measured again. Since the sideband drive leads to heating of the cyclotron mode, in a next step, by repeated cyclotron mode cooling in the precision trap and transport to the analysis trap, a low $n_+ < n_{+,\mathrm{th}}$ state is prepared and the spin state analysed again. From a comparison of the two measured spin states we conclude whether the spin in the precision trap was flipped. By repeating this scheme many times the spin-flip probability P_{SF} as a function of $\nu_{\mathrm{rf,PT}}$ is obtained. Normalizing each applied $\nu_{\mathrm{rf,PT},k}$ by the associated $\nu_{c,k}$ where k is the measurement number, one obtains a so-called g-factor resonance, $P_{SF}(\nu_L/\nu_c)$, with a maximum at $\mu_p/\mu_N = g_p/2$. For the normalization we use the average $(\nu_{c,1} + \nu_{c,2})/2$ of the two cyclotron frequency measurements. This compensates for linear magnetic field drifts which potentially take place while spin transitions are driven.

The result of our g-factor measurement is shown in Fig. 3. Incoherences caused by the coupling of the particle's axial motion to the axial detection circuit in the slightly inhomogeneous magnetic field of the precision trap prevent P_{SF} from exceeding 50% (ref. 16). The linewidth of the measured resonance is 12.5 p.p.b., which is caused by saturation and thermal fluctuations of the modified cyclotron energy E_+. The latter causes fluctuations of the axial frequency, $\nu_{z,\mathrm{PT}} \propto B_2 E_+$, which lead to fluctuations of the measured cyclotron frequency via equation (2), thus contributing to the linewidth. The measured data set is analysed using the maximum-likelihood method[26] based on a Gaussian distribution with the g-factor being the lineshape centre. The maximum-likelihood method is a statistical parameter estimation technique and avoids the need for arbitrary data binning, which may result in a biased estimate of the fitting parameters. From the data analysis we obtain

$$\mu_p = \frac{g_p}{2}\mu_N = 2.792\,847\,348(7)\mu_N$$

where the number in parentheses is the statistical uncertainty of the fit, which corresponds to a relative precision of 2.6 p.p.b.

Systematic shifts $\Delta(g_p/2)$ of the measured $(g_p/2)$ value are caused by time and energy dependencies of ν_L and ν_c

$$\frac{\Delta(g_p/2)}{(g_p/2)} = \frac{\Delta\nu_L(E_+,E_z,E_-,t)}{\nu_L} - \frac{\Delta\nu_c(E_+,E_z,E_-,t)}{\nu_c} \quad (3)$$

The frequency shifts $\Delta\nu_L(E_+, E_z, E_-, t)$ and $\Delta\nu_c(E_+, E_z, E_-, t)$ are caused by trap imperfections such as a slightly inhomogeneous magnetic field at the centre of the precision trap or an anharmonic trapping potential. To first order, the shifts induced by the magnetic field inhomogeneities cancel in the frequency ratio, because they contribute the same relative amount to ν_c and ν_L (refs 4 and 15). A considerable systematic shift can be caused by an anharmonicity of the electrostatic potential that only affects ν_c while ν_L remains unchanged. Thus, the trapping potential was optimized by careful adjustment of the voltages applied to the compensation electrodes of the precision trap to obtain $\Delta\nu_c = 0$. The relative uncertainty in the resulting shift $\Delta\nu_c$ is 0.20 p.p.b. A second g-factor resonance was recorded where the electrostatic potential was deliberately de-tuned to shift the modified cyclotron frequency by –5 p.p.b. Within error, we obtained the same $(g_p/2)$ value, which confirms that systematic shifts due to electrostatic anharmonicities are understood and negligible at the present level of precision. In addition to these two leading-order shifts, relativistic frequency shifts and image-charge shifts contribute[15]. However, because the frequency measurements are carried out in thermal equilibrium with the cryogenic detection system the relativistic shift contributes only at a level of 0.03 p.p.b. For our trap geometry the image-charge shift is −0.088 p.p.b. Thus, both shifts can be neglected. Time-dependent shifts are due to voltage and magnetic field drifts. The effect of voltage drifts was characterized by performing a sequence of axial frequency measurements at constant E_+. The corresponding systematic shift in ν_c is –0.07(0.35) p.p.b.

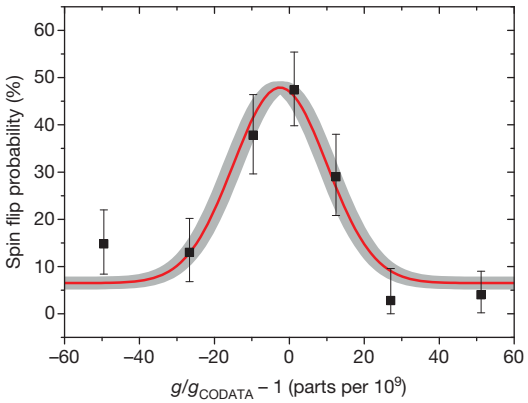

Figure 3 | Measured g-factor resonance. The abscissa is the measured g value normalized to the currently accepted value g_{CODATA}. The solid line is a maximum-likelihood fit to the data, which avoids the need for data binning. The shaded area indicates the 1σ confidence band of the fit. Filled squares representing binned data points with 1σ error bars are shown for visualization and do not explicitly enter the line fit. It took about four months to record the entire set of 450 data points.

The dominant systematic uncertainty is caused by nonlinear drifts of the magnetic field. By comparing the cyclotron frequency measurements before and after application of the spin-flip drive we find an average shift $\nu_{c,2} - \nu_{c,1} = 4$ p.p.b. Such frequency shifts in the precision trap are observed only if the spin-flip drive in the analysis trap has been applied in advance. It is consistent with heating of the electrodes caused by the latter spin-flip drive. Owing to thermal expansion the trap centres are shifted, thereby changing the magnetic field in the precision trap. Once the drive is turned off, thermal relaxation causes the observed drift of the magnetic field. The last contribution considered is a shift of the axial frequency after the measurement of ν_+. The sideband drive heats the particle to a cyclotron energy of $E_+/k_B = T_+ \approx 330$ K, where k_B is the Boltzmann constant. During the subsequent axial frequency measurement, the modified cyclotron mode is cooled resistively. This leads to an effective frequency shift of ν_z and contributes to a shift of the cyclotron frequency by –0.51(0.08) p.p.b. Accordingly, the magnetic moment value is corrected and the final result is

$$\frac{\mu_p}{\mu_N} = \frac{g_p}{2} = 2.792\,847\,350(7)(6) \quad (4)$$

The first and second numbers in parentheses are the statistical uncertainty of the fit and the systematic uncertainty, respectively, see Table 1. The latter is dominated by the nonlinear drift of the magnetic field. The result has a relative precision of 3.3 p.p.b. and is in agreement with the

Table 1 | Error budget of the direct proton *g*-factor measurement

Parameter	Relative shift of $g_p/2$	Uncertainty
Trapping potential	0	0.2×10^{-9}
Relativistic shift	0.03×10^{-9}	-
Image-charge shift	-0.088×10^{-9}	-
Voltage fluctuations	-0.07×10^{-9}	0.35×10^{-9}
Magnetic field relaxation	0	2×10^{-9}
Cyclotron cooling	-0.51×10^{-9}	0.08×10^{-9}
Total systematic shift	-0.64×10^{-9}	2×10^{-9}

This table lists the relative systematic shifts and their uncertainties, which were applied to the measured g_p value.

currently accepted CODATA value $g_{\mathrm{CODATA}}/2 = 2.792847356(23)$, but is 2.5 times more precise.

We expect it will be possible to achieve an improvement in precision by at least another factor of 10, by using an apparatus with reduced residual magnetic field inhomogeneity B_2 in the precision trap, a higher spin-state detection fidelity, as well as by applying phase-sensitive detection techniques[27]. In addition, the so-called Standard Model extension[8] describes diurnal frequency variations as a consequence of violation of the combined charge, parity and time symmetry and Lorentz violation. With faster measurement cycles, which become possible by application of advanced cyclotron cooling techniques, and an improved spin state detection fidelity a search for the predicted effects[28] becomes feasible.

The double Penning-trap method can be applied to measure the antiproton magnetic moment with similar precision[7,29]. A comparison of both values will provide a sensitive test of CPT invariance with baryons. The measurement of the antiproton magnetic moment will be conducted at the BASE experiment[30] at the Antiproton Decelerator of CERN.

Received 6 February; accepted 16 April 2014.

1. Winkler, P. F., Kleppner, D., Myint, T. & Walther, F. G. Magnetic moment of the proton in Bohr magnetons. *Phys. Rev. A* **5,** 83–114 (1972).
2. Häffner, H. *et al.* Double Penning-trap technique for precise *g*-factor determinations in highly charged ions. *Eur. Phys. J. D* **22,** 163–182 (2003).
3. Dehmelt, H. G. & Ekström, P. Proposed *g*-2 experiment on single stored electron or positron. *Bull. Am. Phys. Soc.* **18,** 727–731 (1973).
4. Rodegheri, C. C. *et al.* An experiment for the direct determination of the *g*-factor of a single proton in a Penning trap. *New J. Phys.* **14,** 063011 (2012).
5. DiSciacca, J. & Gabrielse, G. Direct measurement of the proton magnetic moment. *Phys. Rev. Lett.* **108,** 153001 (2012).
6. Karshenboim, S. G. & Ivanov, V. G. The *g*-factor of the proton. *Phys. Lett. B* **566,** 27–34 (2003).
7. DiSciacca, J. *et al.* One-particle measurement of the antiproton magnetic moment. *Phys. Rev. Lett.* **110,** 130801 (2013).
8. Bluhm, R., Kostelecký, V. A. & Russell, N. CPT and Lorentz tests in Penning traps. *Phys. Rev. D* **57,** 3932–3943 (1998).
9. Beringer, J. *et al.* (Particle Data Group). Review of particle physics. *Phys. Rev. D* **86,** 010001 (2012).
10. Van Dyck, R. S. Jr, Farnham, D. L., Zafonte, S. L. & Schwinberg, P. B. High precision Penning trap mass spectroscopy and a new measurement of the proton's "atomic mass". *AIP Conf. Proc.* **457,** 101–110 (1999).
11. Sturm, S. *et al.* High-precision measurement of the atomic mass of the electron. *Nature* **506,** 467–470 (2014).
12. Pohl, R. *et al.* The size of the proton. *Nature* **466,** 213–216 (2010).
13. Van Dyck, R. S., Schwinberg, P. B. & Dehmelt, H. G. New high-precision comparison of electron and positron *g*-factors. *Phys. Rev. Lett.* **59,** 26–29 (1987).
14. Hanneke, D., Fogwell, S. & Gabrielse, G. New measurement of the electron magnetic moment and the fine structure constant. *Phys. Rev. Lett.* **100,** 120801 (2008).
15. Brown, L. S. & Gabrielse, G. Geonium theory: physics of a single electron or ion in a Penning trap. *Rev. Mod. Phys.* **58,** 233–311 (1986).
16. Brown, L. S. Geonium lineshape. *Ann. Phys.* **159,** 62–98 (1985).
17. Ulmer, S. *et al.* Observation of spin flips with a single trapped proton. *Phys. Rev. Lett.* **106,** 253001 (2011).
18. Gabrielse, G. *et al.* Special relativity and the single antiproton: fortyfold improved comparison of $\bar{p}$ and p charge-to-mass ratios. *Phys. Rev. Lett.* **74,** 3544–3547 (1995).
19. Ulmer, S. *et al.* Direct measurement of the free cyclotron frequency of a single particle in a Penning trap. *Phys. Rev. Lett.* **107,** 103002 (2011).
20. Ulmer, S. *et al.* A cryogenic detection system at 28.9 MHz for the non-destructive observation of a single proton at low particle energy. *Nucl. Instrum. Meth. A* **705,** 55–60 (2013).
21. Wineland, D. J. & Dehmelt, H. G. Principles of the stored ion calorimeter. *J. Appl. Phys.* **46,** 919–930 (1975).
22. Mooser, A. *et al.* Demonstration of the double Penning-trap technique with a single proton. *Phys. Lett. B* **723,** 78–81 (2013).
23. Mooser, A. *et al.* Resolution of single spin-flips of a single proton. *Phys. Rev. Lett.* **110,** 140405 (2013).
24. DiSciacca, J., Marshall, M., Marable, K. & Gabrielse, G. Resolving an individual one-proton spin flip to determine a proton spin state. *Phys. Rev. Lett.* **110,** 140406 (2013).
25. Cornell, E. A., Weisskoff, R. M., Boyce, K. R. & Pritchard, D. E. Mode coupling in a Penning trap: π pulses and a classical avoided crossing. *Phys. Rev. A* **41,** 312–315 (1990).
26. Sivia, D. S. & Skilling J. *Data Analysis—A Bayesian Tutorial* 1st edn (Oxford Science, 2010).
27. Sturm, S. *et al. g*-factor measurement of hydrogenlike $^{28}Si^{13+}$ as a challenge to QED calculations. *Phys. Rev. A* **87,** 030501 (2013).
28. Mittleman, R. K., Ioannou, I. I., Dehmelt, H. G. & Russell, N. Bound on CPT and Lorentz symmetry with a trapped electron. *Phys. Rev. Lett.* **83,** 2116–2119 (1999).
29. Smorra, C. *et al.* Towards a high-precision measurement of the antiproton magnetic moment. *Hyperfine Interact.*. doi:10.1007/s10751-014-1018-7 (2014).
30. Ulmer, S. *et al. Technical Design Report BASE* CERN Document Server, SPSC-TDR-002, http://cds.cern.ch/record/1503514?ln=de (CERN, 2013).

Acknowledgements We acknowledge the financial support of the BMBF, and of the EU (ERC grant number 290870-MEFUCO), the Helmholtz-Gemeinschaft, HGS-HIRE, the Max-Planck Society, IMPRS-PTFS, and the RIKEN Initiative Research Unit Program.

Author Contributions S.U., C.C.R., H.K., A.M. and C.L. designed and built the experimental apparatus and the data acquisition system. A.M., C.L. and S.U. took part in the months-long data-taking runs. K.F. and A.M. developed the algorithms for the spin state analysis. A.M., K.F., S.U., C.L. and H.K. analysed the data. S.U., A.M., K.B. and J.W. wrote the initial manuscript, which was then improved and approved by all authors.

Author Information Reprints and permissions information is available at www.nature.com/reprints. The authors declare no competing financial interests. Readers are welcome to comment on the online version of the paper. Correspondence and requests for materials should be addressed to A.M. (mooser@uni-mainz.de).